On-chip THz-frequency tuneable plasmonic circuits

J. Wu[1], A. S. Mayorov, **C. D. Wood**, D. Mistry, L. H. Li, E. H. Linfield, A. G. Davies and J. E. Cunningham

[1]School of Electronic and Electrical Engineering, University of Leeds, Woodhouse Lane, Leeds UK LS2 9JT

Abstract—**We demonstrate the excitation and electrostatic modulation of a planar, resonant plasmonic circuit, comprised of a two-dimensional electron system (2DES) integrated into three different on-chip, terahertz-frequency coplanar waveguides. We utilise a Schottky gate formed across the 2DES in one device to create a resonant cavity in which the carrier concentration, and therefore the cavity resonant frequency, can be tuned by application of a negative DC gate bias, or using an external magnetic field. Using this technique, we demonstrate tuneable plasmon and magnetoplasmon generation and detection at frequencies up to ~ 400 GHz, by injection of terahertz pulses into the 2DES from the waveguide region.**

I. INTRODUCTION

THE use of time-resolved terahertz-frequency (THz) measurements to probe semiconductor systems in which carriers have been confined in one or more dimensions, allows investigation of a range of fundamental physical phenomena which occur on picosecond timescales. Typically, such measurements involve exposing a device containing a two-dimensional electron system (2DES) to coherent, free-space-propagating THz radiation. Information regarding carrier dynamics within the 2DES is inferred either through capture of the transmitted/reflected THz radiation, and/or a rectification response within the 2DES. Such techniques have been used to study, for example, cyclotron emission from a 2DES [1], coupling between cyclotron-transitions within a 2DES and THz metamaterial resonators [2], and the formation of plasmonic crystals using a gate-controlled 2DES [3]. In plasmonic cavity devices with dimensions of a few tens of microns, sub-wavelength confinement results in resonant frequencies which occur in the THz-frequency range. Such devices offer the possibility of fabricating planar, plasmonic circuits that can be used to manipulate THz signals.

In this paper, three different device geometries were fabricated. These were: a capacitively coupled device (D1); an injection device (D2); and a gated injection device (D3). Each device was formed on a 2DES-containing, GaAs/AlGaAs heterostructure (Fig. 1a), grown using molecular-beam-epitaxy on top of a photoconductive (PC) layer of low-temperature-grown (LT-) GaAs. The waveguide in each case was a 50 Ω coplanar waveguide (CPW), comprising a 30-µm-wide centre conductor separated from adjacent ground planes by 20 µm gaps, which was patterned onto the structure using optical lithography. The point at which the CPW was formed depended on the device being formed, as discussed below.

For D1, a 0.8 mm × 5 mm mesa was etched into the wafer surface using citric acid, which terminated on an AlAs etch-stop layer incorporated into the heterostructure during growth, at a depth of ~ 600 nm. A selective HF:H_2O (1:9) wet etch was used to remove the etch-stop layer, and to expose the underlying LT-GaAs PC material. A CPW was then formed across the 2DES-containing mesa, such that the centre conductor and 2DES were separated by the capacitive barrier of the growth heterostructure.

In D2, prior to formation of the large mesa, a 100-nm-high, 73 µm × 25 µm mesa was first formed in the 2DES using a H_2SO_4:H_2O_2:H_2O (1:8:70) non-selective wet etch. Next, 10 × 30 µm AuGeNi contact pads were defined at either end of the 2DES mesa and annealed at ~ 500 °C to form Ohmic contacts to the submerged 2DES. A CPW containing a break in the centre conductor was aligned to overlay the mesa Ohmic contacts (Fig. 1b, excluding the Schottky gate), thereby allowing injection and extraction of guided-wave THz pulses into / out from the integrated low-dimensional system.

D3 was identical to D2 with the exception of a 4.4 µm metal Schottky gate (Ti/Au, 10/60 nm) which was defined across the mesa using electron-beam lithography prior to deposition of the CPW (Fig. 1b).
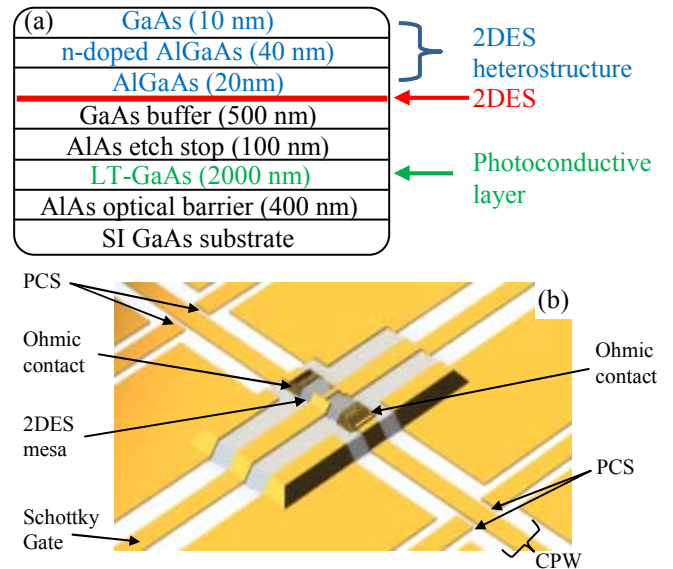

Figure 1: (a) Illustration of the MBE-grown material containing a photoconductive layer for THz excitation and detection, overlaid by a 2DES-containing heterostructure. (b) Schematic of D3, a gated injection device.

II. METHODOLOGY

In all devices, two pairs of shunt bias arms, arranged perpendicularly to the coplanar waveguide and with a separation of 5 µm from the centre conductor, were used to define two photoconductive switch (PCS) pairs which were separated laterally by 1.2 mm and located on either side of the 2DES. THz pulses were excited in the CPW by illumination of a biased PCS using a pulsed Ti:Sapphire laser (100 fs pulsewidth, 80 MHz repetition rate). The quadrature switch arrangement allows the generated THz signal to be detected by

illumination (using a second, time-delayed laser beam) of either the switch directly opposite the excitation switch (the 'input' pulse), or using a switch from the PCS pair located along the waveguide, on the far side of the 2DES (the 'output', or transmitted THz pulse). At the CPW-2DES interface, a portion of the THz signal couples into the 2DES either capacitively (D1), or via the Ohmic contacts (D2 and D3) where it excites a broad spectrum of plasmons whose spectral content (up to a maximum of ~ 400GHz) is limited primarily by radiative losses, and waveguide losses arising from the high permittivity and loss tangent of GaAs-based substrates.

Measurements were taken in a dilution refrigerator, into which dispersion compensated pump and probe NIR laser beams were coupled via two, single-mode solid-core optical fibres [4]. Briefly, the fibres were each terminated inside a pivoted ferrule which allowed control over the direction of the emitted laser beams. Each ferrule position was adjusted using two sets of crossed, linear piezoelectric stage pairs (one pair for each ferrule), allowing micron-precision alignment of each laser beam to the appropriate PCS located on the sample surface below. As well as allowing *in situ* exchange between input and output pulse measurements as required, the dynamic control of laser position allows compensation of thermal drift during cycling of the fridge temperature to be performed prior to detailed measurements. Measurements were taken using 2 mW optical excitation powers, with a PCS bias of 5 V DC.

III. RESULTS

The transmitted signal was detected using two different methodologies: conventional pump-probe techniques, in which the probe laser beam was modulated using an optical chopper, and a gate-modulation technique, in which the overlaid Schottky gate was used to dynamically alter the 2DES carrier density, allowing difference measurements to be performed of the transmitted signal. In devices D1 and D2, the collective plasmon oscillations were detected using the former technique, as we have demonstrated previously [4]. Room temperature measurements of D1 showed no interaction with the capacitively coupled 2DES (corresponding to maximum amplitude transmitted signal) owing its high resistance. Upon cooling, the increasing conductivity of the 2DES created a lossy conductive-plane beneath the CPW with which the THz signal interacted, generating plasmonic waves. At ~ 0.2 K, the highly conductive 2DES (DC resistance ~ 200 Ω) prevented any transmitted THz signal from being detected owing to disruption of the guided mode within the CPW. Upon application of a magnetic field aligned perpendicularly to the plain of the device, cyclotron oscillations excited within the 2DES increased sufficiently its DC resistance such that transmitted THz signals of increasing amplitude could be detected. The bandwidth of the transmitted signal increased linearly with field and the band edge is defined by the cyclotron resonance within the 2DES (Fig. 2a). Unfortunately, no details of sub-cyclotron resonance oscillations, such as magnetoplasmons, were observed owing to poor signal-to-noise caused by disruption of the guided THz mode.

THz signals injected directly into a 2DES were next

measured in D2. By measuring the input and output pulse, we observe both a reduction in THz signal reflected from the 2DES interface (at the Ohmic contact) and a corresponding increase in the transmitted broadband THz signal as a function of reducing temperature (Fig. 2b). However, again owing to high noise levels inherent in these measurements, more interesting information cannot be extracted from the data.
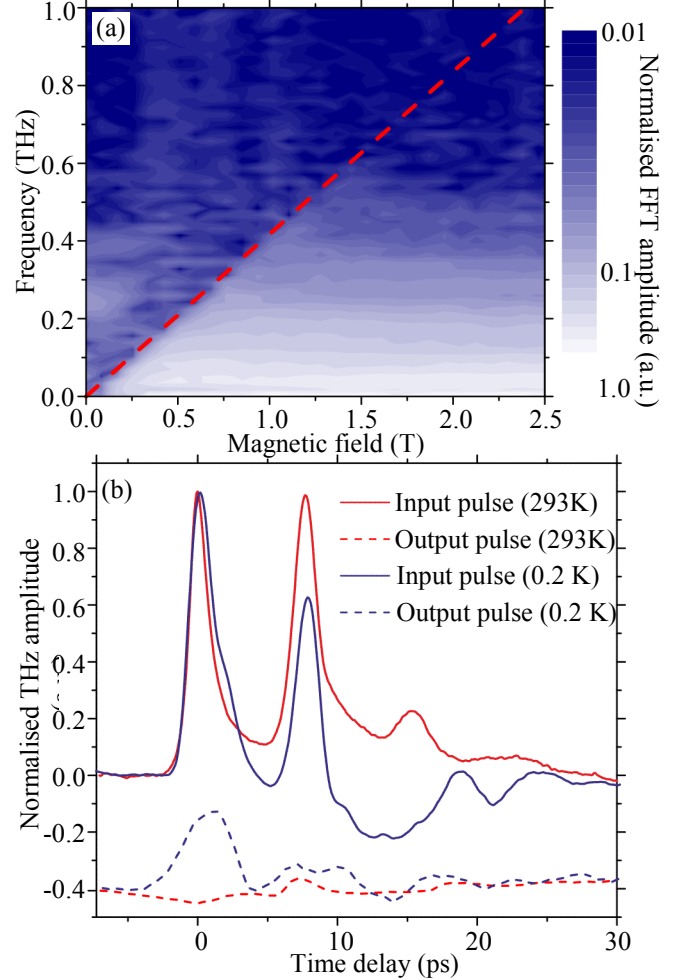

Figure 2: (a) Normalised FFT amplitude of the THz signal as a function of external magnetic field applied perpendicularly to the plane of the device, compared with calculated values for the cyclotron resonance (red dash). (b) input (solid) and output (dashed) THz signals recorded on a device containing an un-gated 2DES at 293 K (red) and 4 K (blue).

Finally, measurements of a gated injection device were performed in D3. The formation of a Schottky gate over the mesa defines two different regions within the 2DES: those for which the carrier concentration is constant, and those for which the carrier concentration can be adjusted by application of a DC gate bias (i.e. directly beneath the gate). The dispersion relation of carriers in the 2DES is given by:

$$\omega_p = \sqrt{\frac{n_s e^2 k}{2m^* \varepsilon_0 \varepsilon_{eff}(k)}} \tag{1}$$

in which $n_s = 6.26 \times 10^{15}$ m^{-2} is the sheet density of the 2DES, e and m^* are the charge and effective mass of electrons in GaAs, ε_0 and ε_{eff} are the vacuum and effective permittivity of the waveguide, and k is the plasmon wave vector. To excite a resonant plasmonic mode, k must satisfy the condition

$k = n\pi/L$, where $n = 1, 2, 3\ldots$, and L is the length of the plasmonic cavity. The phase velocity of plasmons is then obtained using $v_p = \omega_p/k$. In the ungated regions, the 2DES therefore behaves as a dispersive transmission line. In the gated region, however, the metal gate screens the Coulombic restoring force, which reduces the acceleration of electrons driven by the exciting THz electric field, resulting in a lower v_p in comparison with the ungated areas. The gated plasmon dispersion can hence be written:

$$\omega_p = \sqrt{\frac{n_s e^2 k}{m^* \varepsilon_0 [\varepsilon_2 + \varepsilon_1 \coth(kd)]}} \quad (2)$$

where d is the distance between the gate and 2DES and ε_1 and ε_2 are the relative permittivity of AlGaAs and GaAs, respectively. As $kd \to 0$ in equation 2, the term $\varepsilon_2 + \varepsilon_1 \coth(kd) \to \frac{\varepsilon_1}{kd}$ and therefore $\omega_p \propto k$: the gated region therefore supports a dispersionless, TEM mode. Within this region n_s can be tuned by applying a DC gate bias, V_g.

We found that decreasing V_g negatively from 0 V strongly affected the THz signal reflected from the 2DES interface, until channel pinch-off occurred (i.e. the point at which all carriers beneath the gate are depleted) at $V_g = V_{th} = -3$ V (Fig. 3a). This effect arises from the lower v_p in the gated region with respect to the ungated region causing a mismatch in the plasmonic wave vectors $(k = \omega/v_p)$ across the interface. As V_g decreases, n_s and v_p in the gated region also decrease, increasing correspondingly the mismatch in k, which results in the observed increase in reflection amplitude from the interface between the two regions. Once V_g reaches V_{th}, the 2DES is fully depleted and further changes to V_g have no effect. Other contributions to the signal are attributed to direct coupling across the 4.4 μm gate which are therefore unaffected by the gate bias.

The gate bias was next set to a fixed value of -1.6 V, chosen as small changes in voltage around this value produced large changes in the transmitted THz signal. An AC signal (< 100 mV, 87 Hz) superimposed onto the DC gate bias therefore allows difference measurements of the transmitted signal to be made using lock-in detection. Since the signal coupled directly across the 2DES is constant for all gate biases, this contribution to the transmitted signal disappears from the difference measurements allowing measurement of only the plasmonic modes excited beneath the Schottky gate. Under an external magnetic field, magnetoplasmons are formed in the 2DES by coupling of the plasmon and cyclotron modes. The transmitted signals in Fig. 3b exhibit periodic oscillations which correspond to Fabry-Perot resonance of magnetoplasmonic modes that satisfy the boundary conditions of the gated 2DES region. As the field increases, the oscillation period reduces and the plasmon modes blue shift.

IV. CONCLUSIONS

We have demonstrated three on-chip THz devices which allow the excitation, detection and electrostatic manipulation of THz-frequency 2D plasmons. We demonstrated the use of a gate-modulation technique, through which we could observe

the generation of confined 2D plasmons and magnetoplasmons in the gated cavity region. This work not only provides a useful technique with which to study the ultrafast THz response and carrier dynamics of low-dimensional semiconductor structures, but also has potential future application in the development of plasmonic circuits for the manipulation of THz waves.
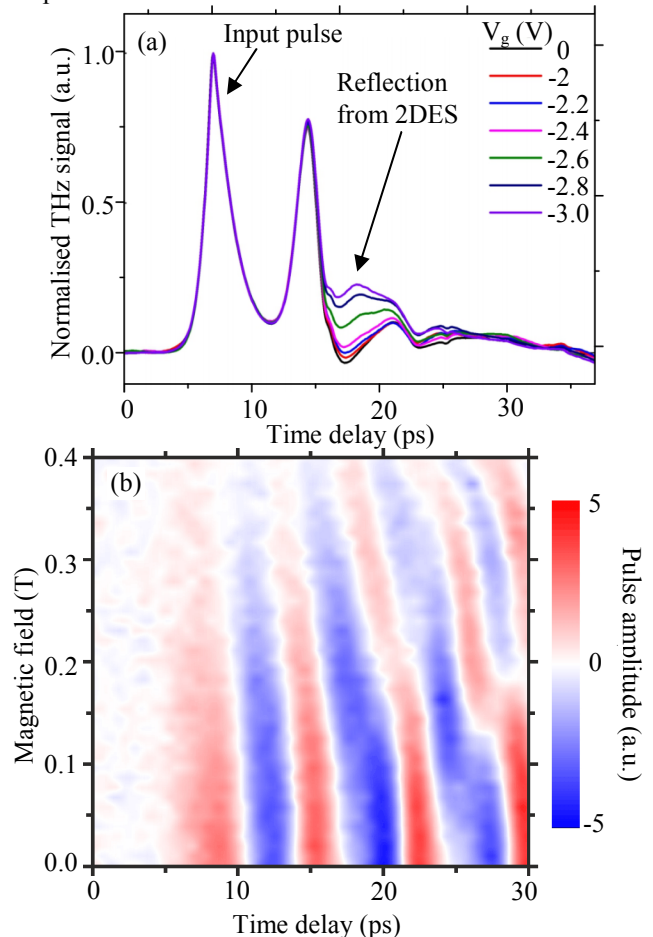

Figure 3: (a) changes in the reflected THz pulse as a function of V_g. (b) Time-domain oscillations in a THz pulse transmitted through a gated 2-DES, caused by plasmon and cyclotron oscillations of carriers function of magnetic field. Measurements were taken at a negative gate bias of -1.6 V.

REFERENCES

[1] X. Wang, D. J. Hilton, L. Ren, D. M. Mittleman, J. Kono, and J. L. Reno, "Terahertz time-domain magnetospectroscopy of a high-mobility two-dimensional electron gas.," *Opt. Lett.*, vol. 32, no. 13, pp. 1845–1847, 2007.
[2] G. Scalari, C. Maissen, D. Turcinkova, D. Hagenmuller, S. De Liberato, C. Ciuti, C. Reichl, D. Schuh, W. Wegscheider, M. Beck, and J. Faist, "Ultrastrong Coupling of the Cyclotron Transition of a 2D Electron Gas to a THz Metamaterial," *Science*, vol. 335, no. 6074, pp. 1323–1326, Mar. 2012.
[3] G. C. Dyer, G. R. Aizin, S. J. Allen, A. D. Grine, D. Bethke, J. L. Reno, and E. A. Shaner, "Induced transparency by coupling of Tamm and defect states in tunable terahertz plasmonic crystals," *Nat. Photonics*, vol. 7, no. 11, pp. 925–930, Sep. 2013.
[4] C. D. Wood, D. Mistry, L. H. Li, J. E. Cunningham, E. H. Linfield, and A. G. Davies, "On-chip terahertz spectroscopic techniques for measuring mesoscopic quantum systems.," *Rev. Sci. Instrum.*, vol. 84, no. 8, p. 085101. Aug. 2013.